LHC dijet constraints on double beta decay

J.C. Helo[*]

Universidad Técnica Federico Santa María,
Centro-Científico-Tecnológico de Valparaíso,
Casilla 110-V, Valparaíso, Chile

M. Hirsch[†]

AHEP Group, Instituto de Física Corpuscular – C.S.I.C./Universitat de València
Edificio Institutos de Investigacion, Parc Cientific de
Paterna, Apartado 22085, E–46071 València, Spain

Abstract

We use LHC dijet data to derive constraints on neutrinoless double beta decay. Upper limits on cross sections for the production of "exotic" resonances, such as a right-handed W boson or a diquark, can be converted into lower limits on the double beta decay half-life for fixed choices of other parameters. Constraints derived from run-I data are already surprisingly strong and complementary to results from searches using same-sign dileptons plus jets. For the case of the left-right symmetric model, in case no new resonance is found in future runs of the LHC and assuming $g_L = g_R$, we estimate a lower limit on the double beta decay half-live larger than 10^{27} ys can be derived from future dijet data, except in the window of relatively light right-handed neutrino masses in the range 0.5 MeV to 50 GeV. Part of this mass window will be tested in the upcoming SHiP experiment. We also discuss current and future limits on possible scalar diquark contributions to double beta decay that can be derived from dijet data.

Keywords: Neutrino mass, Neutrinoless double beta decay, LHC.

---

[*]Electronic address: juancarlos.helo@usm.cl
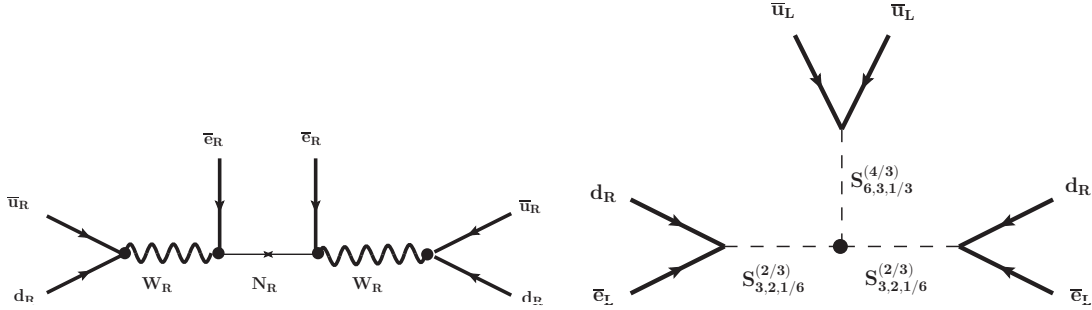[†]Electronic address: mahirsch@ific.uv.es

FIG. 1: Two example diagrams of short-range contributions to double beta decay. To the left: (a) Left-right symmetric model, example of $W_R - N_R - W_R$ exchange ("topology-I" contribution); to the right: (b) a scalar diquark model classified as T-II-4 in [13] ("topology-II" type contribution). For discussion see text.

I. INTRODUCTION

Current experimental data on neutrinoless double beta decay ($0\nu\beta\beta$) give limits for ^{76}Ge [1] and ^{136}Xe [2–4] in the range of $T_{1/2}^{0\nu\beta\beta} \gtrsim (1-2) \times 10^{25}$ ys. Proposals for next generation $0\nu\beta\beta$ experiments even claim $T_{1/2}^{0\nu\beta\beta} \sim 10^{27}$ yr can be reached for ^{136}Xe [5, 6] and ^{76}Ge [7, 8]. Usually, these limits are interpreted in terms of upper limits on Majorana neutrino masses. However, any lepton number violating extension of the standard model will contribute to $0\nu\beta\beta$ decay at some level and exchange of some TeV-scale exotic particles could give even the dominant contribution to the total $0\nu\beta\beta$ decay rate, see for example the recent reviews [9, 10].

The classical example of such a short-range contribution to $0\nu\beta\beta$ decay [11] is the right-handed W-boson exchange diagram in left-right (LR) symmetric models [12], see fig. (1) to the left. Here, N_{R_i} are the right-handed partners of the ordinary neutrinos ν_{L_i}. The general classification of all possible decompositions of the $d = 9$ $0\nu\beta\beta$ decay operator can be found in [13]. In the language of [13], the diagram in fig. (1) left is an example for a topology-I model. Topology-II contributions to $0\nu\beta\beta$ decay, on the other hand, introduce no new fermions. To choose one particular example for T-II from the list of [13] we take T-II-4, BL#11. Here, BL# 11 refers to operator $\mathcal{O}_{11}$ in the list of effective $\Delta L = 2$ operators of [14]. This model introduces a scalar diquark, $S_{DQ} \equiv S_{6,3,1/3}$[1], and a leptoquark, $S_{LQ} \equiv S_{3,2,1/6}$. The short-range diagram contributing to $0\nu\beta\beta$ decay in this model is shown in fig. (1) on the right. We will come back to discuss more details of diquarks in $0\nu\beta\beta$ decay in the next section. Here, we only mention in passing that a possible $SU(5)$ embedding of this model has been recently discussed in [15].

At pp-colliders the classical signal of lepton number violation (LNV) is the final state

---

[1] Here and everywhere else in this paper subscripts denote the transformation properties/charge under the standard model gauge group, $SU(3)_c \times SU(2)_L \times U(1)_Y$.

with two same-sign leptons plus two jets and no missing energy ($lljj$). This signal was first discussed in the context of left-right symmetric models in [16], where it can be simply understood as reading the diagram in fig. (1), from left to right. Both, ATLAS [17] and CMS [18] have searched for this signal and give upper limits on $\sigma \times Br$ as a function of the resonance mass. [2] These limits can then be converted into excluded regions in parameter space for different models. For the example of the left-right symmetric model, for right-handed neutrino masses, m_{N_R}, of the order of $m_{N_R} \simeq \frac{1}{2} m_{W_R}$, this leads to very strong lower limits on m_{W_R} of the order of $m_{W_R} \gtrsim (2.7 - 3)$ TeV [17, 18], assuming $g_R = g_L$. However, these limits deteriorate rapidly if right handed neutrinos are relatively light ($m_{N_R} \lesssim 100$ GeV) or heavy ($m_{N_R} \gtrsim m_{W_R} - 100$ GeV). In the former case, the lepton and the jets emitted in the decay of N_R are highly boosted and thus the lepton is no longer isolated, failing one of the basic selection criteria used by both LHC collaborations. If, on the other hand, m_{N_R} approaches m_{W_R}, the jets and the lepton from the N_R-decay become to soft to pass elementary p_T-cuts. Finally, for $m_{N_R} \gtrsim m_{W_R}$, N_R contributes only off-shell to the decay of W_R and the branching ratio for the decay $W_R \to lljj$ drops to unmeasurably small values.

One can use ATLAS [17] and CMS [18] limits to constrain also all other models with short-range contributions to the $0\nu\beta\beta$ decay rate. Diquarks have particularly large cross sections at the LHC [19], so in the kinematic region where $m_{S_{LQ}} < m_{S_{DQ}}/2$ constraints from the $lljj$ search can be expected to be even more severe than for LR models. Contributions to $0\nu\beta\beta$ decay from leptoquark models, on the other hand, are less constrained from LHC data. In [20, 21] current limits and expected sensitivities based on the $lljj$ search for run-II have been discussed for all T-I decompositions in the list of [13].

ATLAS [22] and CMS [23] have searched for heavy, narrow resonances decaying to pairs of jets. No clear signal for any new state has been found and both collaborations provide upper limits on production cross sections times branching ratio as function of the unknown resonance mass. These limits can be converted into an upper limit on the unknown coupling of the resonance to quarks (or, less interesting for us: gluons) as a function of the resonance mass. In this paper, we discuss how these limits can be used to constrain short-range contributions to $0\nu\beta\beta$ decay, despite the fact that no LNV is searched for in the dijet data. As we discuss below, the limits we derive are complementary to the limits derived from the $lljj$ search and are surprisingly strong already with only run-I data. We also estimate future LHC sensitivities and their implications for $0\nu\beta\beta$ decay. In our numerical analysis, we concentrate on the two example models, shown in fig. (1), but also comment briefly on other possible contributions to $0\nu\beta\beta$ decay.

The rest of this paper is organized as follows. In section II we repeat very briefly the basics of the two models, which we use as examples. Section III gives our numerical results. We then close in section IV with a short discussion.

---

[2] In the CMS data there is an excess around $(2 - 2.2)$ TeV with a 2.8 σ c.l. local significance. The ATLAS data, however, does not confirm this excess. We thus consider it a statistical fluctuation.

II. MODEL BASICS

Our general arguments will apply to any ($\Delta L = 2$) model containing an exotic scalar or vector, which couples to a pair of quarks. For definiteness, we use the following two examples: (1) The minimal left-right symmetric model and (2) a scalar diquark model. In this section we briefly recall the basics of these two setups.

A. Left-right symmetry

The minimal left-right symmetric model extends the standard model gauge group to $SU(3)_C \times SU(2)_L \times SU(2)_R \times U(1)_{B-L}$ [12, 24, 25] and assigns both left- and right-handed fermion fields as doublets (under left and right groups, respectively). Thus the model contains necessarily three generations of right-handed neutrinos. Charged and neutral current interactions of the new gauge bosons are given by

$$\mathcal{L} = \frac{g_R}{\sqrt{2}} \left(V_{ud}^R \cdot \bar{d}\gamma^\mu P_R u + V_{lN}^R \cdot \bar{l}\gamma^\mu P_R N \right) W_{R\mu}^- \tag{1}$$
$$+ \frac{g_R}{\sqrt{1 - \tan^2\theta_W (g_L/g_R)^2}} Z_{LR}^\mu \bar{f}\gamma_\mu \left[T_{3R} + \tan^2\theta_W (g_L/g_R)^2 (T_{3L} - Q) \right] f,$$

Here, V_{lN}^R (V_{ud}^R) is the right-handed sector lepton (quark) mixing, g_L, g_R are the gauge couplings and θ_W is the Weinberg angle. Eq.(1) shows that the couplings of the Z' boson to fermions becomes non-perturbative, if $g_R \lesssim g_L \tan\theta_W \simeq 0.35$. Very often in the literature it is assumed that $g_R = g_L$, a special case which we will call manifest left-right symmetry. However, in the numerical section we will allow g_R also to vary.

In the minimal LR model, Majorana masses for the right-handed neutrinos are generated by the vacuum expectation value breaking the $SU(2)_R \times U(1)_{B-L}$ symmetry. One thus expects naively that the $m_{N_{R_i}}$ are of the same order as the right-handed W-boson mass, albeit times an unknown Yukawa coupling. To be as general as possible, however, we will let these masses float freely. The half-life $T_{1/2}$ for $0\nu\beta\beta$ decay via heavy W_R and heavy N_i exchange can then be written as:

$$T_{1/2}^{-1} = G_{01} \left| \sum_i \left(V_{eN_i}^R \right)^2 m_{N_{R_i}} \mathcal{M}(m_{N_{R_i}}) \times \frac{m_{W_L}^4}{m_{W_R}^4} \frac{g_R^4}{g_L^4} \right|^2 \tag{2}$$

Here, $\mathcal{M}(m_{N_{R_i}})$ is a nuclear matrix element, which depends on $m_{N_{R_i}}$, and G_{01} is the leptonic phase space integral. We will use the numerical values of [26] for $\mathcal{M}(m_{N_{R_i}})$ in our analysis. For $m_{N_{R_i}}$ larger than approximately $p_F \simeq \mathcal{O}(0.1 - 0.2)$ GeV, $\mathcal{M}(m_{N_{R_i}}) \propto \frac{1}{m_{N_{R_i}}^2}$ and we define the "effective right-handed neutrino mass" as

$$\frac{1}{\langle m_N \rangle} = \sum_i \left(V_{eN_i}^R \right)^2 \frac{1}{m_{N_{R_i}}}. \tag{3}$$

Note that due to the presence of Majorana phases there can be cancellations among terms in $\langle m_N \rangle$, which could lead to vastly larger values of the half-live but never to a shorter one

compared to the case without Majorana phases. The latter is important, when deriving lower limits on $T_{1/2}$ from LHC data.

For our analysis the exact fit to neutrino oscillation data is unimportant. However, for completeness we mention that the minimal LR model can explain this data at tree-level via the seesaw mechanism [27–30]. Naive expectation gives heavy-light neutrino mixing in the seesaw as $V \propto \sqrt{m_\nu/M_N}$, i.e. $|V_{l4}|^2 \simeq 5 \times 10^{-14}(\frac{m_\nu}{0.05\text{eV}})(\frac{1\text{TeV}}{M_{N_R}})$. Thus, barring immensely huge cancellations among different contributions to m_ν, for an ordinary seesaw in LR models one expects that N decays through a W_R to $l^\pm jj$, with nearly equal rates in l^+ and l^-, with a branching ratio close to 100 %.

B. Scalar diquarks

As the second example model we discuss scalar diquarks. We define scalar diquarks as particles coupling to a pair of same-type quarks. They can be either colour triplets or sextets. In the context of $0\nu\beta\beta$ decay, diquark contributions were first discussed in [31, 32]. A systematic list of all (scalar) diquark contributions to $0\nu\beta\beta$ decay was given in [13]. We will concentrate on one particular diquark model for definiteness. Constraints on other models will be very similar; we will comment briefly in the numerical section.

From the list of possible diquark decompositions [13], we choose the example T-II-4, BL# 11. This particular case introduces a diquark $S_{DQ} \equiv S_{6,3,1/3}$ plus a leptoquark $S_{LQ} \equiv S_{3,2,1/6}$, see fig. (1). The Lagrangian of the model can be written as

$$\mathcal{L}_{DQLQ} = \mathcal{L}_{SM} + g_1\bar{Q} \cdot \hat{S}_{DQ} \cdot Q^C + g_2\bar{L} \cdot S_{LQ}^\dagger d_R + \mu S_{LQ}S_{LQ}S_{DQ}^\dagger + \text{h.c.} \tag{4}$$

For convenience we introduced the notation $\hat{S}_{DQ} = S_{DQ,a}^{(6)}(T_{\bar{\mathbf{6}}})_{IJ}^a$, with $I, J = 1 - 3$ and $a = 1 - 6$ the color triplet and sextet indexes, respectively. The symmetric 3×3 matrices $T_{\mathbf{6}}$ and $T_{\bar{\mathbf{6}}}$ can be found in ref. [13]. g_1 and g_2 are dimensionless Yukawas, we suppress generation indices for brevity. μ has dimension of mass. Note that the Lagrangian in eq. (4) necessarily violates lepton number by two units.

$0\nu\beta\beta$ decay is generated via the diagram in fig. (1), to the right. Since neither diquarks nor leptoquarks can have masses light compared to the nuclear Fermi scale, this diagram is always of the short-range type. The inverse half-life is then

$$T_{1/2}^{-1} = G_{01}\left|\epsilon_{DQ}\mathcal{M}_{DQ}\right|^2, \tag{5}$$

where [13]

$$\mathcal{M}_{DQ} = \frac{1}{48}\mathcal{M}_1 - \frac{1}{192}\mathcal{M}_2 \tag{6}$$

with $\mathcal{M}_{1,2}$ as defined in [11], where numerical values for ^{76}Ge can be found, for other isotopes see [9]. ϵ_{DQ} is given by

$$\epsilon_{DQ} = \frac{2m_p}{G_F^2} \frac{g_1 g_2^2 \mu}{m_{DQ}^2 m_{LQ}^4}. \tag{7}$$

The model under consideration does not contain any right-handed neutrino, instead it generates neutrino masses at 2-loop order [33]. Since for our purposes the exact numerical fit to neutrino data is not important, we will not discuss the details here. See either [34] for a general discussion of 2-loop neutrino mass models and/or [32], where a very similar diquark model (based on a down-type diquark) has been discussed in more details.

III.   NUMERICAL RESULTS

We use CalcHEP [35] to calculate the cross section for W_R production and MadGraph5 [36] for the calculation of the x-section of the diquark. We have checked against existing results in the literature [19] and found good agreement. We will first discuss our results for the left-right symmetric model.

For deriving the constraints we use the CMS [23] data. ATLAS [22] data leads to very similar results. Moreover, for estimating the future sensitivities, we make use of the fit of the SM dijet distribution fitted to a Monte Carlo simulation as given in ref. [37]. We then have estimated future limits coming from dijet searches for an assumed luminosity of $\mathcal{L} = 300$ fb^{-1}.

A.   Left-right symmetric model

The branching ratio of the decay of a W_R boson into two jets can be calculated as a function of its mass, once the masses of the right-handed neutrinos are fixed. In our numerical calculation we take into account decays of the W_R to fermions. [3] For masses of $m_{N_{R_i}} > m_{W_R}$ and $m_t \ll m_{W_R}$, $Br(W_R \to jj)$ then reaches approximately $Br(W_R \to jj) \simeq 2/3$. For all $m_{N_{R_i}} \ll m_{W_R}$, $Br(W_R \to jj) \simeq 1/2$ for $m_t \ll m_{W_R}$. Using our calculated cross section $\sigma(pp \to W_R)$, the $Br(W_R \to jj)$ and the upper limits on production cross sections times branching ratio from dijet searches at $\sqrt{s} = 8$ TeV and $\mathcal{L} = 19.7$ fb^{-1} given by ref. [23] we have then calculated limits for g_R as function of m_{W_R} for the LR model. Upper limits ranging from roughly $g_R \sim [0.25, \sqrt{4\pi}]$ result for m_{W_R} in the range $m_{W_R} \simeq [1.2, 4.4]$ TeV.

For the sake of simplicity consider first the case of manifest LR symmetry, i.e., $g_R = g_L$, first. In Fig. 2(a) we show two limits from the non-observation of $0\nu\beta\beta$. The gray region on the left is ruled out by $0\nu\beta\beta$, corresponding to a half life $T_{1/2} = 1.9 \times 10^{25}$ yr [1, 2], while the stronger limit (blue region) corresponds to an expected future sensitivity of $T_{1/2} = 10^{27}$ yr. Note that plots for ^{136}Xe sensitivities are very similar. The yellow region in the top corner shows CMS current limits from searches of like-sign leptons plus two jets at $\sqrt{s} = 8$ TeV and $\mathcal{L} = 19.7$ fb^{-1} [18]. Due to the choice of a logarithmic axes for m_N, this region seems to represent only a tiny part of the parameter space. However, we remind the reader that the

---

[3] Decays of the W_R to SM bosons depend on the mixing angle between W_R and SM W boson [38], which we assume is small for simplicity.
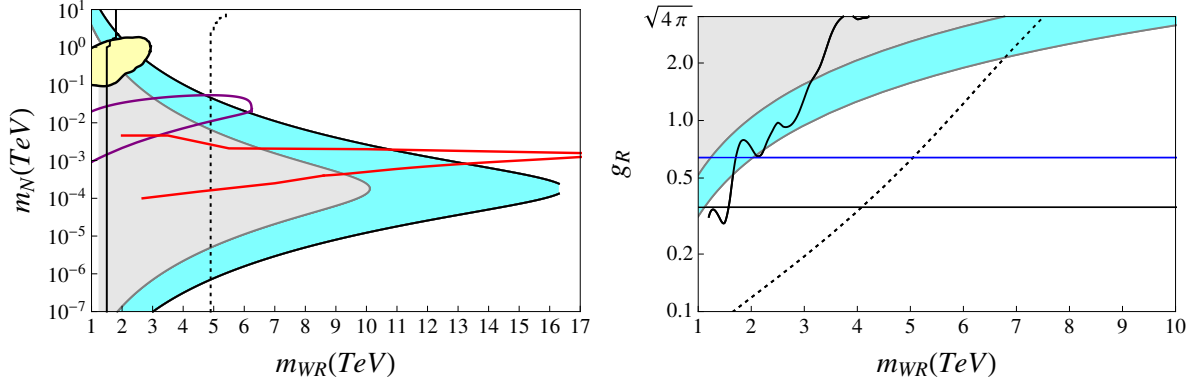
FIG. 2: Regions in parameter space, which can be probed by dijet (black, full/dashed lines) and like sign leptons plus two jets (yellow region) searches at LHC, displaced vertex search at LHC (inside the purple lines), SHiP (red lines) and $0\nu\beta\beta$ decay. (a) Left: m_{W_R} vs m_{N_R} for fixed $g_R = g_L$ (b) Right for fixed $m_N = 1$ TeV as a function of g_R. The black full (dashed) line are current (estimated future) LHC limits. The gray region is the current lower limit in $0\nu\beta\beta$ decay half-life of ^{76}Ge, the blue one the estimated future sensitivity of $T_{1/2} = 10^{27}$ ys. For more details see text.

naive expectation for m_N is typically $m_N \sim \mathcal{O}(m_{W_R})$. The solid red line in the middle of the plot shows the region in the parameter space, which can be probed by heavy neutrino searches at the upcoming SHiP experiment [39, 40]. The solid purple line shows the region in parameter space where a displaced vertex search at the LHC could yield at least 5 events at $\sqrt{s} = 13$ TeV and $\mathcal{L} = 300$ fb^{-1} [41, 42]. The nearly vertical solid (dotted) lines correspond to current (future) LHC limits from dijet searched at $\sqrt{s} = 8$ TeV (13 TeV) and $\mathcal{L} = 19.7$ fb^{-1} (300 fb^{-1}). The lines for the dijet limits assume three degenerate right-handed neutrinos of mass m_N. If only one right-handed has a mass below m_{W_R}, the branching ratio Br($W_R \to jj$) increases, leading to stronger limits from the dijet search.

Current searches of like-sign leptons plus two jets have imposed a lower limit at $m_{W_R} \gtrsim (2.7 - 3.0)$ TeV in the neutrino mass range 0.1 TeV $\lesssim m_{N_R} \lesssim 2.0$ TeV [4]. For this part of the parameter region, the LHC limits rule out already a dominant LR short-range contribution to $0\nu\beta\beta$. The current dijet searches impose a lower limit at $m_{W_R} \simeq 1.5$ TeV (2.0 TeV) for $\forall m_{N_{R_i}} < m_{W_R}$ ($\forall m_{N_{R_i}} > m_{W_R}$). As can be seen from Fig. 2(a), dijet limits are complementaries to those coming from like-sign leptons plus two jets, extending the range also to the case $m_{N_R} > m_{W_R}$ and to $m_{N_R} \lesssim 100$ GeV, although for such "light" right-handed neutrinos dijet searches are not yet competitive with $0\nu\beta\beta$ decay limits.

Future dijets searches will impose strong limits at $m_{W_R} \lesssim 5$ TeV in case no new resonance is found at 13 TeV and $\mathcal{L} = 300$ fb^{-1}. As can be seen from Fig. 2(a) these limits will leave only a small window for LR short-range contribution for $0\nu\beta\beta$ experiments with half-lives of order 10^{27} (10^{25}) ys at right-handed neutrino masses around $1/2$ MeV $\lesssim m_{N_{R_i}} \lesssim 50$ GeV

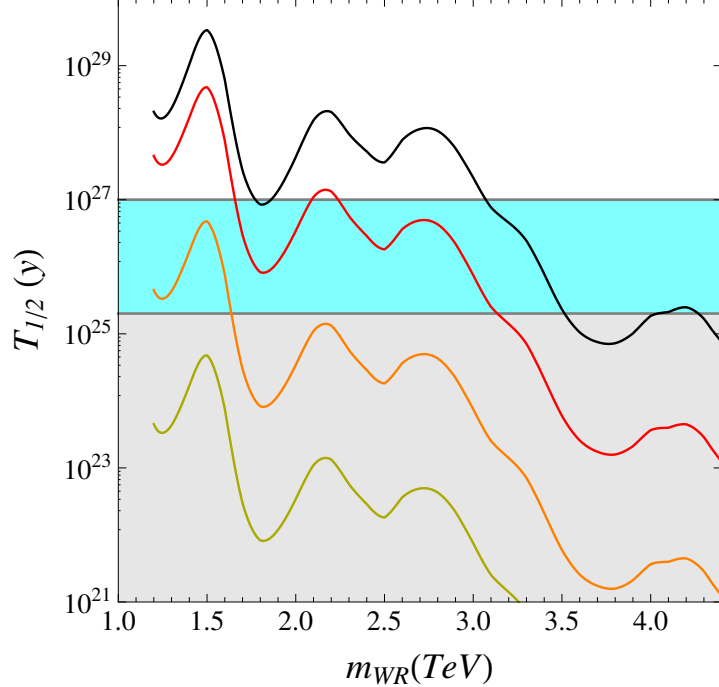[4] These limits are expected to be extended up to $m_{W_R} = 5$ TeV in future searches [43]

FIG. 3: Lower limit on the $0\nu\beta\beta$ decay half-life of ^{76}Ge, derived from LHC dijet data for the left-right symmetric model for different values of the effective right-handed neutrino mass. The gray region is the current lower limit in $0\nu\beta\beta$ decay half-life of ^{76}Ge, the blue one the estimated future sensitivity of $T_{1/2} = 10^{27}$ ys. From top to bottom: $\langle m_N \rangle = m_{W_R}$, $\langle m_N \rangle = 1$, 0.1 and 0.01 TeV. For $\langle m_N \rangle \geq m_{W_R}$ half-lives below the experimental limit (straight line) are ruled out for values of m_{W_R} up to 3.5 TeV. For $m_{W_R} \simeq 4.4$ TeV current LHC data do no longer give any constraint (the LHC limit on g_R reaches $\sqrt{4\pi}$).

(5 MeV $\lesssim m_{N_{R_i}} \lesssim 7$ GeV). Part of this window will be covered by SHiP (in the region of heavy neutrino masses $m_{N_{R_i}} \sim 1-2$ GeV) and a possible displaced vertex search [39, 41, 42].

In Fig. 2(b) we drop the assumption of manifest LR symmetry. Here we show, just as in Fig. 2(a), a comparison between the $0\nu\beta\beta$ and dijet searches at LHC, but for fixed heavy neutrino mass $m_{N_R} = 1$ TeV in the plane $g_R - m_{W_R}$. The blue horizontal line corresponds to the choice $g_R = g_L$. The black horizontal line corresponds to the limit $g_R \lesssim g_L \tan\theta_W \simeq 0.35$ where the Z' coupling to fermions becomes non perturbative, as is explained in section II. As shown, and in agreement with the previous analysis, dijet searches are competitive to $0\nu\beta\beta$ for $m_{N_R} = 1$ TeV, especially for small values of g_R. For this choice of m_{N_R}, future $0\nu\beta\beta$ decay data can compete with future LHC dijet data only for values of g_R close to the non-perturbative limit.

Having fixed the limit on g_R as function of m_{W_R}, we can then calculate lower limits for half-lives for $0\nu\beta\beta$ decay, for different assumed values of $\langle m_N \rangle$. Examples are shown for the case of ^{76}Ge in fig. (3) using current LHC dijet limits. Note that the plots extend up to $m_{W_R} \simeq 4.4$ TeV; at this point the limit on g_R becomes worse than $g_R \simeq \sqrt{4\pi}$, and the theory would be non-perturbative, i.e. the limits no longer have any physical meaning. For $\langle m_N \rangle = m_{W_R}$

the strongest lower limits result, for the whole region of m_{W_R} up to $m_{W_R} \simeq 3.5$ TeV half-life limits longer than the current experimental limit can be derived. The constraints become less stringent for smaller values of $\langle m_N \rangle$ and are practically completely irrelevant for masses lower or equal than $\langle m_N \rangle \simeq 10$ GeV using current LHC data.

We close this discussion with a short comment on charged scalars. Decompositions with singly charged scalars appear in the list of short-range $0\nu\beta\beta$ decay contributions [13]. The cross section of S_+ at the LHC is typically around a factor of 2 smaller than the cross section for a heavy W', for the same value of the coupling constants to quarks. Thus, similar albeit slightly weaker limits, as discussed here for W_R, can be derived from dijet searches also for charged scalar contributions to $0\nu\beta\beta$ decay. One slight complication arises for charged scalars, however, with respect to the LR model discussed here: In a gauge model, like LR, the coupling of W_R to quarks and leptons is universal, whereas for the charged scalar the couplings $g_{ud}(\bar{u}d)S_+$ and $g_{eN}(\bar{e}N)S_+^\dagger$ could in principle be different. If $g_{ud} \neq g_{eN}$ the discussion for charged scalars will resemble more the case of scalar diquarks, which we discuss next.

B. Scalar diquark Model

Now we turn to the results for the scalar diquark model. As in the LR symmetric case we have used the cross section $\sigma(pp \to S_{DQ})$ and the $Br(S_{DQ} \to jj)$ to calculate current and future limits from dijet searches, using the upper limits on production cross sections times branching ratio from dijet searches [23]. For estimating future sensitivities we use the estimated QCD backgrounds from the Monte Carlo simulation [37].

For the sake of simplicity we will assume the Yukawa couplings g_1 and g_2 are different from zero for the first quark and lepton generations only. In this model the scalar diquark has two possible decay modes: two jets (jj) and two lepton plus two jets $(lljj)$. On one hand, in the parameter region $m_{DQ} < 2m_{LQ}$ the $Br(S_{DQ} \to jj) \simeq 1$ since S_{LQ} contributes only off-shell to the decay of $S_{DQ} \to S_{LQ}^* S_{LQ}^* \to lljj$ and the $Br(S_{DQ} \to lljj)$ drops to unmeasurably small values. On the other hand, in the region where $m_{LQ} << m_{DQ}$ the $Br(S_{DQ} \to jj)$ becomes a function of also m_{LQ} and the (unknown) parameters μ and g_2, see eq.(4).

Consider first the simpler case $m_{LQ} \geq m_{DQ}/2$. In Fig. 4 we show two limits from the non-observation of $0\nu\beta\beta$. The gray region on the left is ruled out by $0\nu\beta\beta$, corresponding to a half life $T_{1/2} = 1.9 \times 10^{25} yr$ [1, 2], while the stronger limit (blue region) corresponds to an expected future sensitivity of $T_{1/2} = 10^{27} yr$. The solid (dotted) lines correspond to current (future) LHC limits from dijet searched at $\sqrt{s} = 8$ TeV (13 TeV) and $\mathcal{L} = 19.7$ fb^{-1} (300 fb^{-1}). Double beta decay limits were calculated using, in Eq. (7), $m_{LQ} = m_{DQ}$, $\mu = m_{DQ}$, $g_2 = 1$(left) and $m_{LQ} = m_{DQ}$, $\mu = \sqrt{4\pi} \, m_{DQ}$, $g_2 = \sqrt{4\pi}$ (right). For larger masses m_{LQ} or smaller couplings g_2 and μ those limits become weaker. Note that the case $g_2 \equiv g_1$, which is more similar to the case of the LR symmetric model, where uinversality of couplings is enforced by the gauge symmetry, $0\nu\beta\beta$ sensitivities would be much worse than
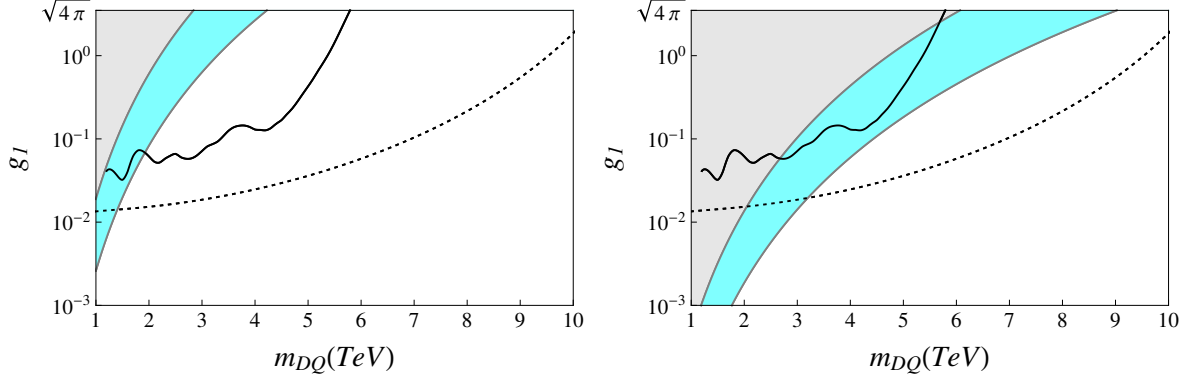
FIG. 4: Future and current limits from dijet searches at LHC compared with double beta decay experiments. The gray region on the top left corner is ruled out by $0\nu\beta\beta$. The blue region corresponds to an expected future sensitivity of $T_{1/2} = 10^{27} yr$. The solid (dotted) black line correspond to current (future) limits from dijet searches. The $0\nu\beta\beta$ limits were calculated using $m_{LQ} = m_{DQ}$, $g_2 = 1$ (left), $\sqrt{4\pi}$ (right) and $\mu = m_{DQ}$ (left), $\sqrt{4\pi}\, m_{DQ}$ (right).
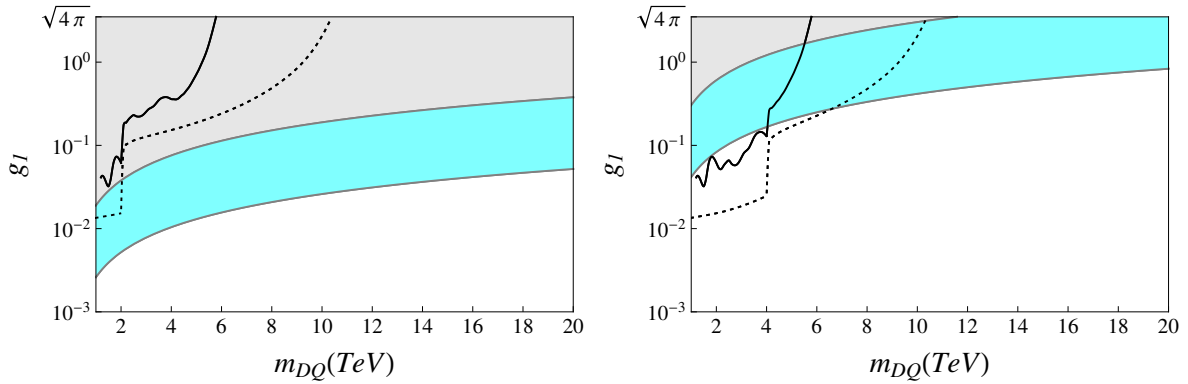

FIG. 5: Future and current limits from dijet searches at LHC compared with double beta decay experiments. The gray region on the top left corner is ruled out by $0\nu\beta\beta$. The blue region corresponds to an expected future sensitivity of $T_{1/2} = 10^{27} yr$. The solid (dotted) black line correspond to current (future) limits from dijet searches. The $0\nu\beta\beta$ and LHC limits were calculated using for $\mu = m_{DQ}$, $g_2 = 1$ and $m_{LQ} = 1\ TeV$ (left), $2\ TeV$ (right).

the ones shown in this plot. Already with current LHC data, dijet limits are more stringent than current $0\nu\beta\beta$ decay limits in this part of parameter space, except for a window of very small values of g_1 at small m_{DQ}. The large reach of the LHC simply reflects the large diquark production cross section.

In Fig. 5 we show, just as in Fig. 4, a comparison between the $0\nu\beta\beta$ and dijet searches at LHC, but for $\mu = m_{DQ}$, $g_2 = 1$, $m_{LQ} = 1$ TeV (left), and $m_{LQ} = 2$ TeV (right). Smaller values of m_{LQ} give $0\nu\beta\beta$ decay a better sensitivity to g_1, while for these relatively large values of μ the diquark has sizeable branching ratio into $lljj$ final states, thus reducing the LHC sensitivity in the dijet search. As fig. 5 shows, in this part of the parameter space the

dijet search can not fully compete with $0\nu\beta\beta$ decay. However, since this reduced sensitivity comes from the competition between $lljj$ and jj final states, one can expect that this part of the parameter space can be covered with future lepton number violating searches at the LHC. We plan to come back to study this part of parameter space in more detail in a future publication on topology-II $0\nu\beta\beta$ decay.

We close this section with a short comment on charged scalars and other types of diquarks. Down-type diquarks have cross sections roughly a factor $\sim (4-8)$ smaller than the up-type diquarks discussed here, with charged scalars having smaller cross sections still [21]. Thus, numerically weaker limits from dijet searches are expected for these cases. However, the discussion for these cases will be similar qualitatively. Therefore, we do not repeat all details for charged scalars and down-type diquarks here.

IV. SUMMARY

We have discussed how upper limits on dijet cross sections, derived from LHC data, can be used to constrain the short-range part of the $0\nu\beta\beta$ decay amplitude. We have concentrated on two example models: (a) minimal left-right symmetry and (b) a diquark model with LNV. For both setups, the LHC dijet data [22, 23] provides constraints complementary to those derived from the search for $lljj$ final state [17, 18]. We have also estimated the impact of future LHC data. Current dijet limits provide already interesting constraints on $0\nu\beta\beta$ decay, future limits will rule out measurably "small" half-lives of double beta decay ($T_{1/2} \lesssim 10^{27}$ ys), except in some well-defined regions of parameter space. The details for the different cases are discussed in the main text. We note that, while we have concentrated on two particular example models, similar constraints will apply to any short-range contribution to $0\nu\beta\beta$ decay in which a state coupling to a pair of quarks appars.

Finally, we note that dijet data can give interesting limits on $0\nu\beta\beta$ decay, as long as no new physics is found in the search. If, however, a new resonance were to appear in the data of run-II, obviously dedicated $\Delta L = 2$ searches will be needed to prove or disprove any connection of such a hypothetical discovery to $0\nu\beta\beta$ decay. In this sense, dijet searches are complementary to the "standard" $lljj$ search at the LHC, but can not replace it as a discovery tool.

[1] GERDA Collaboration, M. Agostini et al., Phys.Rev.Lett. **111**, 122503 (2013), arXiv:1307.4720.

[2] EXO-200 Collaboration, J. Albert et al., Nature **510**, 229234 (2014), arXiv:1402.6956.

[3] KamLAND-Zen Collaboration, I. Shimizu, Neutrino 2014, Boston (2014).

[4] KamLAND-Zen Collaboration, A. Gando et al., Phys. Rev. Lett. **110**, 062502 (2013), arXiv:1211.3863.

[5] KamLAND-Zen Collaboration, A. Gando et al., Phys.Rev. **C85**, 045504 (2012), arXiv:1201.4664.

[6] EXO-200 Collaboration, D. Auty, Recontres de Moriond, http://moriond.in2p3.fr/ (2013).

[7] GERDA Collaboration, I. Abt et al., (2004), arXiv:hep-ex/0404039.

[8] Majorana Collaboration, C. Aalseth et al., Nucl.Phys.Proc.Suppl. **217**, 44 (2011), arXiv:1101.0119.

[9] F. F. Deppisch, M. Hirsch, and H. Päs, J.Phys. **G39**, 124007 (2012), arXiv:1208.0727.

[10] M. Hirsch, AIP Conf. Proc. **1666**, 170007 (2015).

[11] H. Päs, M. Hirsch, H. Klapdor-Kleingrothaus, and S. Kovalenko, Phys.Lett. **B498**, 35 (2001), arXiv:hep-ph/0008182.

[12] R. N. Mohapatra and G. Senjanovic, Phys. Rev. **D23**, 165 (1981).

[13] F. Bonnet, M. Hirsch, T. Ota, and W. Winter, JHEP **1303**, 055 (2013), arXiv:1212.3045.

[14] K. Babu and C. N. Leung, Nucl.Phys. **B619**, 667 (2001), arXiv:hep-ph/0106054.

[15] R. M. Fonseca and M. Hirsch, Phys. Rev. **D92**, 015014 (2015), arXiv:1505.06121.

[16] W.-Y. Keung and G. Senjanovic, Phys.Rev.Lett. **50**, 1427 (1983).

[17] ATLAS, G. Aad et al., (2015), arXiv:1506.06020.

[18] CMS, V. Khachatryan et al., Eur.Phys.J. **C74**, 3149 (2014), arXiv:1407.3683.

[19] T. Han, I. Lewis, and Z. Liu, JHEP **1012**, 085 (2010), arXiv:1010.4309.

[20] J. Helo, M. Hirsch, S. Kovalenko, and H. Päs, Phys.Rev. **D88**, 011901 (2013), arXiv:1303.0899.

[21] J. Helo, M. Hirsch, H. Päs, and S. Kovalenko, Phys.Rev. **D88**, 073011 (2013), arXiv:1307.4849.

[22] ATLAS, G. Aad et al., Phys.Rev. **D91**, 052007 (2015), arXiv:1407.1376.

[23] CMS, V. Khachatryan et al., Phys.Rev. **D91**, 052009 (2015), arXiv:1501.04198.

[24] J. C. Pati and A. Salam, Phys.Rev. **D10**, 275 (1974).

[25] R. Mohapatra and J. C. Pati, Phys.Rev. **D11**, 2558 (1975).

[26] M. Hirsch, H. Klapdor-Kleingrothaus, and O. Panella, Phys.Lett. **B374**, 7 (1996), arXiv:hep-ph/9602306.

[27] P. Minkowski, Phys.Lett. **B67**, 421 (1977).

[28] T. Yanagida, Conf.Proc. **C7902131**, 95 (1979).

[29] M. Gell-Mann, P. Ramond, and R. Slansky, Conf.Proc. **C790927**, 315 (1979), Supergravity, P. van Nieuwenhuizen and D.Z. Freedman (eds.), North Holland Publ. Co., 1979.

[30] R. N. Mohapatra and G. Senjanovic, Phys. Rev. Lett. **44**, 912 (1980).

[31] P.-H. Gu, Phys.Rev. **D85**, 093016 (2012), arXiv:1101.5106.

[32] M. Kohda, H. Sugiyama, and K. Tsumura, Phys.Lett. **B718**, 1436 (2013), arXiv:1210.5622.

[33] J. Helo, M. Hirsch, T. Ota, and F. A. P. Dos Santos, JHEP **1505**, 092 (2015), arXiv:1502.05188.

[34] D. Aristizabal Sierra, A. Degee, L. Dorame, and M. Hirsch, JHEP **1503**, 040 (2015),

arXiv:1411.7038.

[35] A. Pukhov, (2004), arXiv:hep-ph/0412191.

[36] J. Alwall et al., JHEP **1407**, 079 (2014), arXiv:1405.0301.

[37] P. Richardson and D. Winn, Eur. Phys. J. **C72**, 1862 (2012), arXiv:1108.6154.

[38] J. Brehmer, J. Hewett, J. Kopp, T. Rizzo, and J. Tattersall, (2015), arXiv:1507.00013.

[39] S. Alekhin et al., (2015), arXiv:1504.04855.

[40] SHiP, M. Anelli et al., (2015), arXiv:1504.04956.

[41] J. C. Helo, M. Hirsch, and S. Kovalenko, Phys. Rev. **D89**, 073005 (2014), arXiv:1312.2900.

[42] O. Castillo-Felisola, C. O. Dib, J. C. Helo, S. G. Kovalenko, and S. E. Ortiz, Phys. Rev. **D92**, 013001 (2015), arXiv:1504.02489.

[43] A. Ferrari et al., Phys.Rev. **D62**, 013001 (2000).